For this reason, C at any given temperature is considerably higher in hydrogen than in air.

Figure 2–12 illustrates the dramatic span (logarithmic scale) of possible burning velocities of a given fuel/air mixture, using propane/air as an example. The concentration ranges for detonation are somewhat narrower than for turbulent combustion, which are in turn somewhat narrower than that for laminar burning. Table 2–8 gives some figures illustrating this.

Table 2–8 Comparison of Composition Limits for Laminar Burning and Detonation for Two Combustible Gases Mixed with Air[a]

Fuel	Limits for laminar flames [vol.% in air]		Detonability limits* [vol.% in air]	
	Lower	Upper	Lower	Upper
Acetylene	2.5	100	4.2	50
Hydrogen	4.0	75	18.3	59

a. *Source*: Data from Table 2–2 and H. H. Freytag, *Handbuch der Raumexplosionen.* Verlag Chemie, Weinheim, Germany. (1965): 74.

2.2 Ignition of Premixed Gas/Vapor and Air

2.2.1 Introduction

This section concentrates mainly on initial cloud conditions of normal atmospheric pressure and temperature, and on ignition of pre-mixed hydrocarbon gases and air. Experimental evidence elucidating the basic features of various ignition processes and practical guidelines for prevention of ignition in industrial process plants are considered.

The phrase *ignition source* is used as a general term embracing all categories of heat source that may, in principle, give rise to ignition. The phrase *effective ignition source* indicates that a particular source will actually cause ignition if brought into contact with the specific explosive atmosphere of concern.

Numerous national and international standards and guidelines are currently in place for preventing accidental ignition of explosive atmospheres. In Europe, a comprehensive standard was drafted by CEN

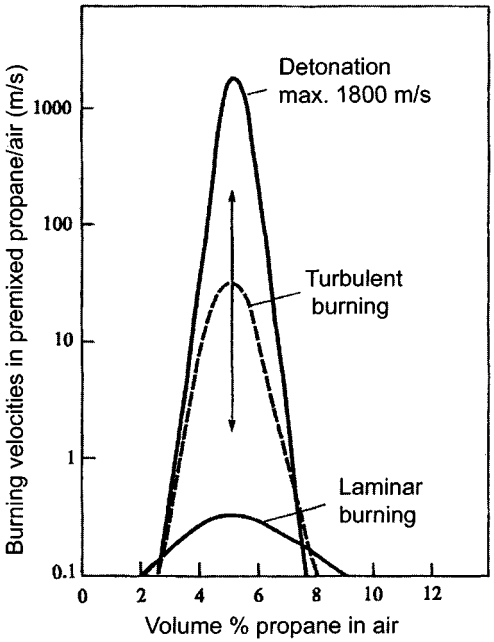

Figure 2–12 Burning velocities in premixed propane/air at atmospheric pressure and normal temperature, for different combustion modes (laminar, turbulent, detonation).

(1993). The document also addresses ignition prevention, and in this context refers to and builds on a series of European and fully international standards on various specific aspects of the ignition prevention problem. The guidelines for industrial practice given in the various sections that follow are mainly based on this document. In addition to Eckhoff (1996), a main source for this section is the paper by Eckhoff and Thomassen (1994).

2.2.2 What Is Ignition? The Basic Theory of "Thermal Runaway"

Explosive gas mixtures can be ignited by a variety of ignition sources including:

- open flames (matches, welding and soldering flames etc.)
- glowing or smoldering materials

- hot solid surfaces
- burning metal particles and "thermite" flashes from impacts, grinding etc.
- electrical and electrostatic sparks, arcs, and other discharge forms
- jets of hot combustion gases
- adiabatic compression
- light radiation, e.g. light conveyed through optical fibers or cables

The question then arises whether ignition by all these quite different sources can be described qualitatively by one common global conceptual model. The answer is yes, and the model is the classical thermal explosion theory formulated by Frank-Kamenetskii (1955). In the following the essence of this theory will be outlined qualitatively with reference to Figure 2–13. In principle the theory applies to any combustible system exposed to a potential ignition source or process. In the context of the present book it applies with equal validity to explosive clouds of combustible gases, liquid sprays/mists, or dusts, and to combustible dust layers/deposits.

Consider an explosive gas mixture, e.g. 4 vol.% propane in air, initially at room temperature. Then consider a small "ignition volume" inside the bulk of this mixture. Assume that the ignition volume can be heated to any desired temperature by a small heating source, e.g. an electrically heated resistance wire that has been placed inside it. Then make the simplifying assumptions that the temperature throughout the ignition volume is uniform at any time during the heating-up process, with a very sharp temperature drop to ambient temperature at the boundary, and that the ignition volume does not expand during heating. Figure 2–13 then illustrates the increase of the heat generation rate inside the ignition volume due to the chemical reaction of the gas mixture there, as well as the increase of the conductive heat loss rate from this volume to the ambient atmosphere, with increasing temperature in the ignition volume.

First, consider the solid lines representing an ignition volume V. The curved line then represents the rate of heat generation G(T) within the ignition volume due to the exothermal reaction between the fuel and the air, as a function of the temperature in this volume. According to the classical Arrhenius theory, this relationship is exponential for a zero-order chemical reaction. The straight solid line represents the rate of heat loss L(T), which increases linearly with the temperature drop between the ignition volume and the ambient gas. Figure 2–13 illustrates that at modest temperatures T the rates of heat generation by combustion are normally substantially

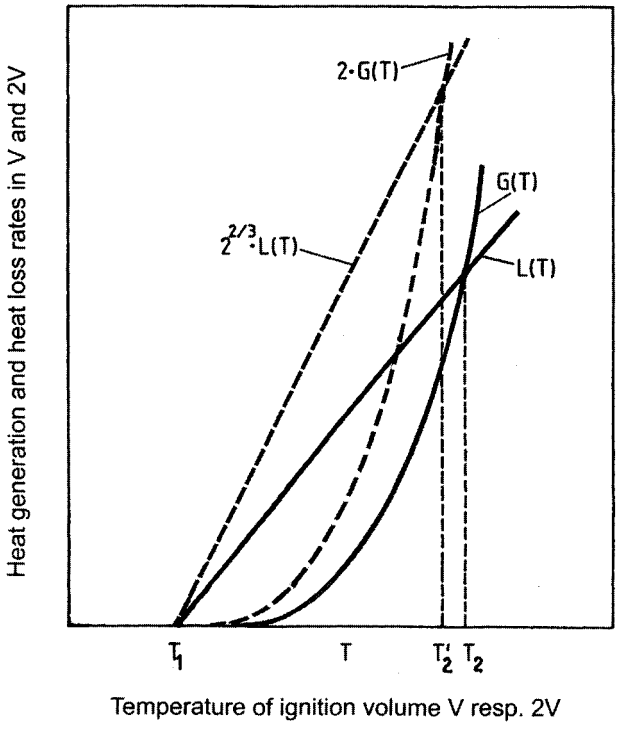

Figure 2–13 Simplified schematic illustration of the basic idea of the "thermal explosion theory" by Frank-Kamenetskii (1955).

lower than the heat loss rates, and it is thus impossible for the temperature in the ignition volume to rise above the ambient temperature T_1 by the slow heat-producing chemical reaction only.

However, if T is raised by activating the external heating source, G(T) will start to raise exponentially. If the external heating is brought to an end while the temperature of the ignition volume is still below the critical temperature for ignition T_2, the rate of heat loss L(T) will still exceed the heat generation rate by chemical reaction G(T), and the temperature in the ignition volume will drop back to ambient temperature again. If, however, T is raised further to a point where G(T) exceeds L(T), a positive feed back loop is established by which further temperature rise is accomplished by the combustion reaction itself. This process will eventually lead to ignition. The critical temperature T_2 for ignition is the one at which:

$$G(T) = L(T) \tag{2.8}$$

and

$$dG(T)/dT > dL(T)/dT \tag{2.9}$$

Now consider the dotted lines in Figure 2–13, representing an ignition volume of 2V. In this case the value of G(T) will be twice that for the ignition volume V for any value of T, simply because the amount of reactive mixture has been doubled. However, because the heat loss rate from the ignition volume increases proportionally with the surface area of this volume, and not with the volume itself, L(T) at any T has only increased by a factor of $2^{2/3}$ compared with the factor of 2 for the ignition volume V. Because of this, the critical temperature T_2' at the crossing point between G(T) and L(T), will be lower in the case of 2V than in the case of V.

This indicates that the minimum temperature that an ignition source must have to cause ignition will decrease with increasing size of the ignition volume to be associated with that source. In reality the shape of the ignition volume will also play an important role.

2.2.3 Ignition by Open Flames and Hot Gases

Open flames are gaseous combustion reactions at temperatures of at least 1000°C. Flames and their hot gaseous reaction products, even at very small volumes, are among the most effective ignition sources for explosive gas clouds.

2.2.4 Ignition by Hot Surfaces

2.2.4.1 Overview

The minimum hot surface temperature for igniting a given mixture of combustible gas in air has sometimes been regarded as a fundamental constant for that mixture. However, this is a false perception. In general terms, ignition is a dynamic process where chemical heat generation and physical heat loss compete in a complex manner in the potential ignition region, and where the former eventually overtakes the latter. This also applies to hot surface ignition.

The size of the hot surface and the relative movement between the explosive gas mixture and the hot surface are two key parameters controlling the minimum ignition temperature, T_{min} of a given gas mixture. Classical investigations of these effects are illustrated in Figure 2–14 and Figure 2–15. Both these experiments should be compulsory background in any study of hot surface ignition processes. The results by Silver (1937) and Paterson (1939, 1940) are shown in Figure 2–14, from which two systematic trends can be extracted

- T_{min} decreases with increasing sphere diameter
- T_{min} decreases with decreasing sphere velocity

There was no significant difference between spheres of quartz and aged platinum.

A similar set of classical results obtained by Mullen et al. (1949) is shown in Figure 2–15.

In this case, an explosive pentane/air mixture was flowing past a stationary hot metal rod at comparatively high velocities. The minimum rod temperature for ignition was recorded as a function of rod diameter and gas velocity. Figure 2–15 reveals the same main trends as Figure 2–14. T_{min} decreases systematically with increasing size of the hot surface and with decreasing relative velocity between the hot surface and the gas. It should be noted that the range of relative velocities is considerably higher in Figure 2–15 than in Figure 2–14, by a factor of about 10.

This strong dependence of T_{min} on actual experimental circumstances is exposed further when comparing values for identical gas mixtures determined in different laboratory test apparatus. Müffling (1946) performed such a comparison and grouped the apparatuses in eight categories as follows:

(a) The explosive gas mixture is passed through a tube of known internal wall temperature.

(b) The mixture is admitted to a vessel of known internal wall temperature.

(c) The mixture is compressed adiabatically and T_{min} is calculated from the lowest compression ratio that gives ignition.

(d) The combustible gas and the air are preheated separately to the desired test temperature and subsequently mixed.

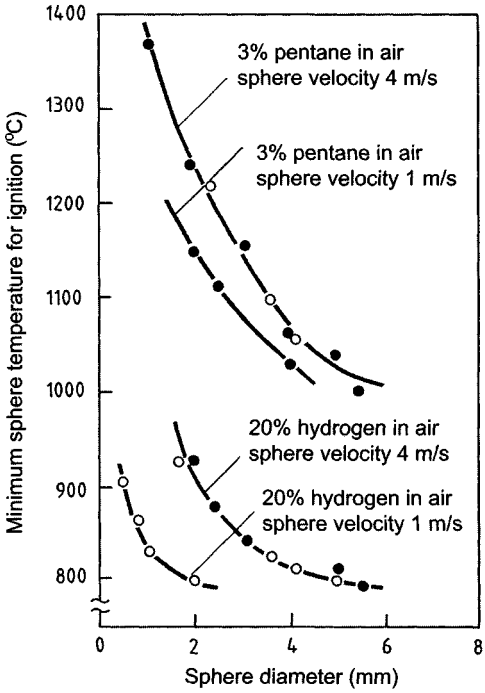

Figure 2–14 Ignition of explosive gas mixtures by hot solid spheres injected into the gas, showing the influence of sphere diameter and velocity on minimum sphere temperature for ignition: (•) quartz spheres; (°) spheres of aged platinum. From Silver (1937) and Paterson (1939, 1940).

(e) A jet of the combustible gas is injected into a vessel containing air preheated to the desired test temperature.

(f) Cool explosive mixture is admitted to a soap bubble surrounding a hot platinum wire of known surface temperature.

(g) A hot solid body of known surface temperature is dropped or ejected into cool explosive mixture.

(h) A hot solid rod of known surface temperature is inserted into cool mixture.

Müffling (1946) reported some results for 7 vol.% hexane in air, showing that method (c) gave a T_{min} of only 300°C, whereas method (d) gave a

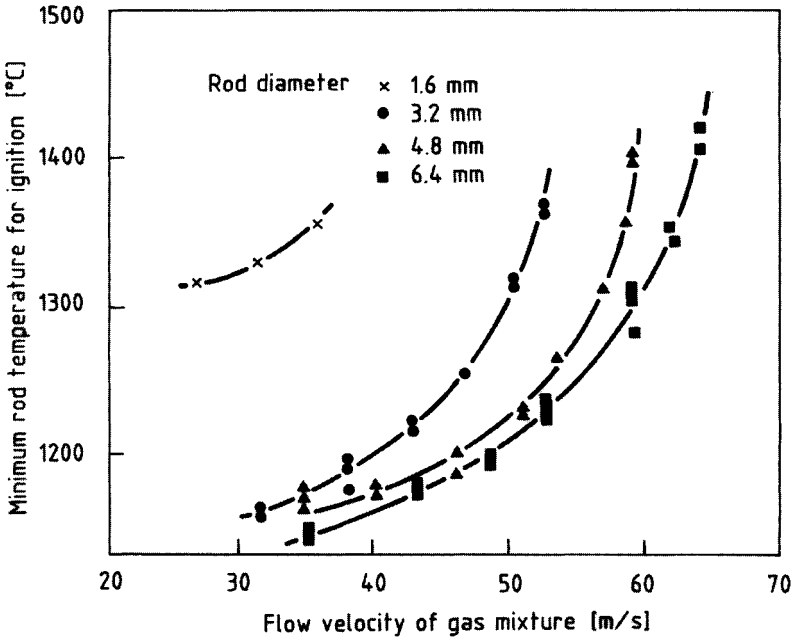

Figure 2–15 Ignition of flowing stoichiometric pre-mixed pentane/air by hot stationary metal rods inserted into a gas flow, showing the influence of the rod diameter, and the gas velocity in relation to the rod, on the minimum rod temperature for ignition. From Mullen et al. (1949).

value of 630°C. For 4–5 vol.% heptane in air the corresponding values were 280°C and 580°C, respectively. The difference of about 300°C in both cases is substantial.

Laurendeau (1982) summarized some more recent published experimental and theoretical work on hot surface ignition of various fuel/air mixtures, with the main emphasis on methane/air. The general validity of the overall trends exhibited by Figure 2–14 and Figure 2–15 was confirmed.

In a subsequent investigation, Alfert and Fuhre (1988) ignited propane/air mixtures in the apparatus shown in Figure 2–16.

After covering the top of the box by a sheet of aluminum foil, making provision for two gas outlet tubes, the box was flushed gently with a propane/air mixture of the desired composition, entering the box through the inlet in the bottom of the box. The rise of fuel concentration in the box

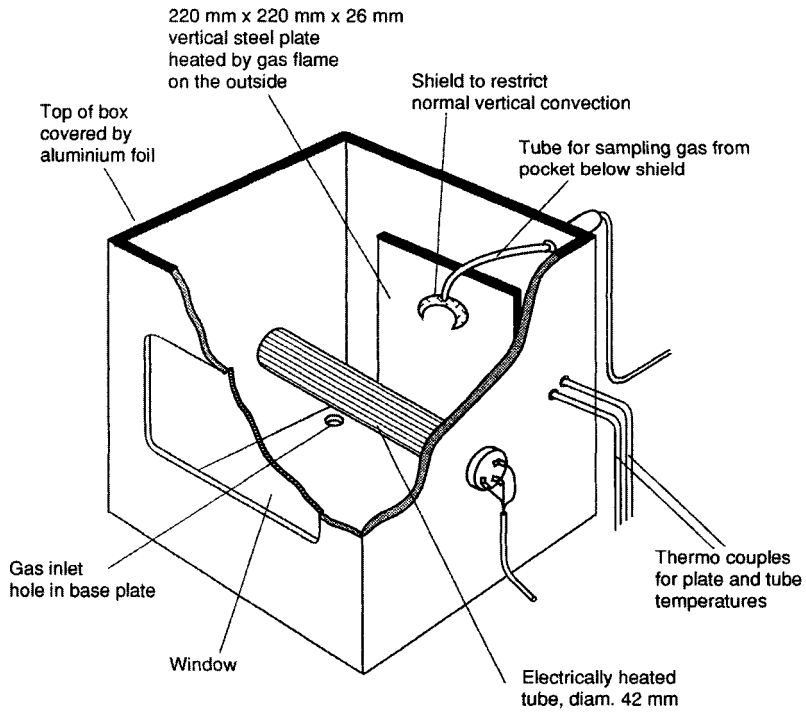

Figure 2–16 Sketch of 50 liter explosion box used for determining minimum ignition temperatures for propane/air under various conditions. In addition to the gas inlet, holes for gas concentration and gas temperature measurement probes were also provided in the base plate. From Alfert and Fuhre (1988).

was monitored continuously. The hot surface was generated when the overall fuel concentration approached the inlet concentration.

When the hot surface temperature reached 600°C, the heating rate was reduced to generate a surface temperature increase of a few degrees per minute. Corresponding values of the hot surface temperature and the propane concentration in the box were recorded at the moment of ignition, the latter being in the range of 4.5–5.0 vol.% in most of the experiments.

The results are summarized in Figure 2–17 and compared with data obtained using the two standard test methods ASTM (2003) and IEC (1975), and a closed bomb method described by Kong et al. (1995).

The results from the experiments in the apparatus shown in Figure 2–16 were from 300°C to 500°C higher than those obtained in the three conservative flask/bomb tests, including the current standard ASTM (2003) and IEC (1975) tests for minimum ignition temperature. This discrepancy calls for a reconsideration of the general applicability of results from current methods of standardized testing for T_{min}.

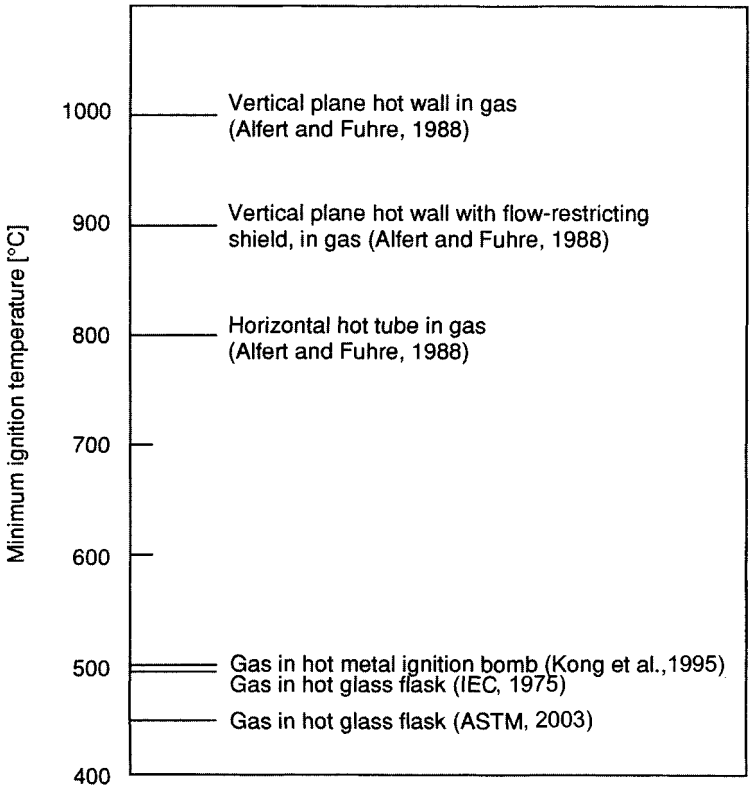

Figure 2–17 Minimum hot surface ignition temperatures for a propane/air mixture at atmospheric pressure, determined by different methods.

2.2.4.2 Minimum Ignition Temperatures of Multi-Component Fuels in Air

In offshore oil and gas production, minimum ignition temperatures of mixtures of multi-component fuels and air are often of interest. For example, natural gas is a multi-component fuel, containing higher hydrocarbons in addition to the methane. For mixtures of methane, propane and

air Kong et al. (1995) investigated the dependence of the ratio of propane/methane on T_{min} of the mixtures. Figure 2–18 shows a significant non-linear decrease of T_{min} with increasing propane/methane ratio. In the hot-bomb method used, a very high equivalence ratio Φ of 2.3 gave a significantly lower T_{min} than for $\Phi = 1$, i.e., for stoichiometric mixtures.

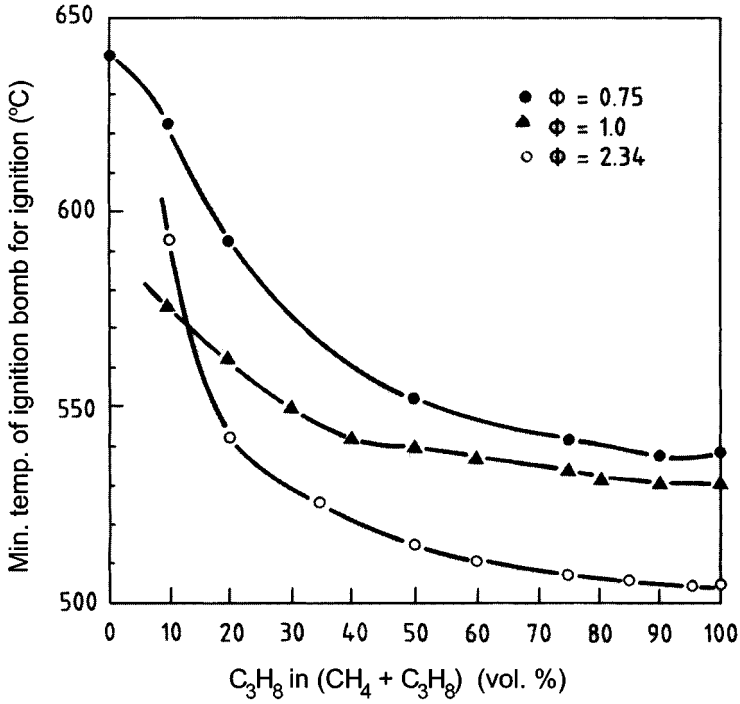

Figure 2–18 Influence of fuel composition on the minimum ignition temperature of CH_4/C_3H_8/air mixtures, for three different overall equivalence ratios Φ, where $\Phi = 1$ for a stoichiometric fuel/air mixture, and $\Phi < 1$ and $\Phi > 1$ represents lean and rich mixtures respectively. From Kong, Eckhoff, and Alfert (1995).

2.2.4.3 Solution for the Future: Dynamic Computer Simulation Models of Hot Surface Ignition

There is a need to reconsider current practices for assessing T_{min} of explosive gaseous fuel/air mixtures for the purpose of process design. A differentiated approach should be developed, which allows critical ignition

conditions to be predicted for both mono- and multi-component fuels, for different geometric hot surface configurations, and for the conditions of heat and gas flow that actually occur in the industrial situation of concern.

The likely approach for the future will be development of comprehensive numerical models containing sub-models of both chemical kinetics and transport processes. Because of the rapid development of fast computers and advanced methods of measurements, reaction kinetics modeling is progressing at great pace. Simulation of fuel oxidation by considering elementary reaction steps has shown good agreement with experimental results.

Integration of a full chemical kinetics package into a mathematical model for predicting T_{min} in practical process situations may be too ambitious at the outset. Using semi-empirical approximations of the influence of chemistry could be a more realistic point of departure. From this perspective, the work of Oberhagemann (1989) is interesting. He developed a semi-empirical model by which T_{min} for single organic components in air can be computed on the basis of the molecular structure of the fuel. Using this model, he computed T_{min} for 380 different organic fuels and correlated with experimental values obtained by the standard IEC (1975) method. The coefficient of correlation was 0.97, corresponding to a mean deviation between experiment and theory of about 10°C. Oberhagemann extended his model to mixtures of two, three, and four different fuels and air, and obtained good correlation with experimental values even in these cases.

2.2.4.4 Standard Test Methods for T_{min}

The current international standard test apparatus used for determining the T_{min} value of explosive gas mixtures for practical explosion prevention is shown in Figure 2–19. However, this is a quite conservative method, as illustrated in Figure 2–17.

In spite of the two standard methods IEC (1975) and ASTM (2003) being very conservative, they may not produce the absolute minimum values that can be found for any given fuel/air mixture. This is because T_{min} determined by closed, isothermal vessel methods of this type decrease somewhat with increasing vessel size. Hence, tests in significantly larger isothermal vessels than the comparatively small vessels used in the two standard methods may yield somewhat lower T_{min} than those obtained with the standard methods.

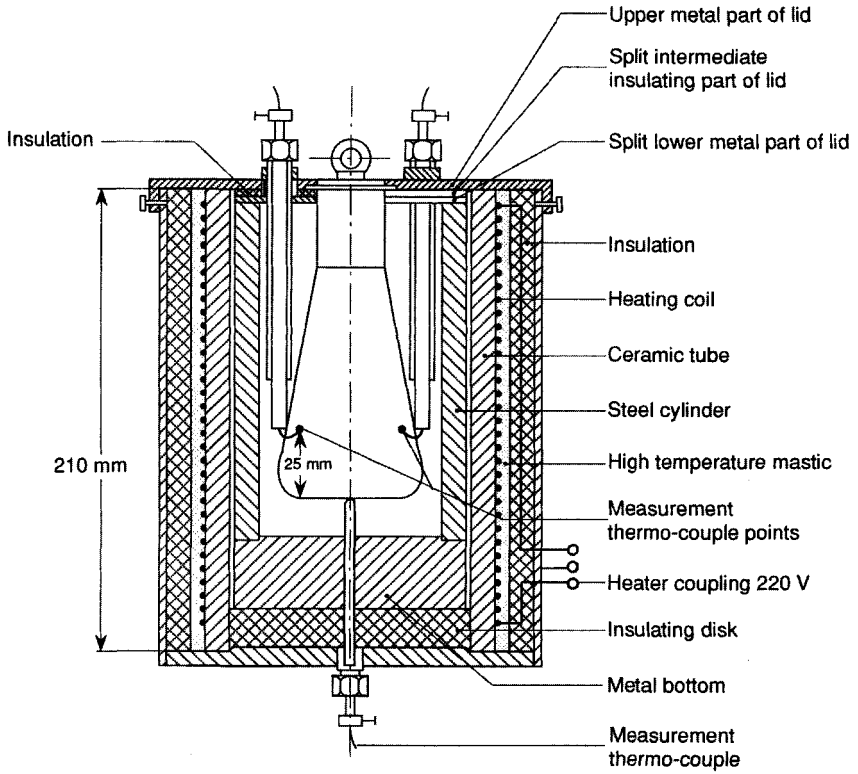

Figure 2–19 The IEC standard 200 cm^3 glass flask apparatus for determining the T_{min} values of explosive mixtures of combustible gases and vapors with air.

2.2.5 Ignition by Burning Metal Particles, "Thermite" Reactions, and Transient Hot Spots

2.2.5.1 Introductory Overview

In the past, the initiation of accidental gas explosions was sometimes attributed to "friction sparks" without any further explanation. However, this imprecise term covers a multifarious category of potential ignition sources, comprising mechanical hot-work operations such as grinding and cutting, repeated impacts on one spot, and single impacts. However, in all these cases, the ignition source is generated by transformation of mechanical energy (impact and friction) into heat.

Existing knowledge suggests that the probability of ignition of a combustible gas-in-air mixture by a mechanical impact is determined by a set of basic parameters characterizing the impact and a set of basic parameters characterizing the gas mixture. Key parameters of the impact include

- chemical composition of colliding bodies
- surface topography of colliding bodies at areas of contact
- contact area
- contact pressure
- sliding velocity parallel to the contact surface
- sliding distance (or contact time)

Key parameters of the gas include

- chemical composition of the fuel gas
- concentrations of fuel, oxygen and inert gas
- dynamic state of the gas (turbulence and systematic velocity components, which are also influenced by the impact process itself)
- temperature
- pressure

Depending on the circumstances, the actual ignition source produced by the impact/friction process is generally either the small hot particles released during the process or the hot spot generated on one or both of the colliding bodies during the impact. In special situations where metals such as aluminum or titanium are involved in the impact together with rust, the impact can generate very incendiary "thermite" flashes due to exothermic transfer of oxygen from the rust to the aluminum or titanium (see Section 2.2.5.3).

2.2.5.2 Ignition by Small Burning Metal Particles from Single Impacts

Small flying hot particles from single impacts between chemically inert materials (rock and other inert minerals) cannot ignite explosive gas mixtures. This is because the mechanically generated temperature rise will not reach the high levels required for such small particles to become an

ignition source. However, if metals are involved in the impact, small metal particles may be torn or cut away from the main bulk and heated mechanically to such an extent that they start to burn spontaneously while flying through the air. Then the particle temperature will increase substantially due to the release of chemical energy. Such small burning metal particles are the genuine "friction sparks".

Much work has been carried out to assess the possibility of igniting methane/air ("firedamp") in coal mines by coal-picking equipment impacting on rock. This is essentially a single-impact process. Research over many years has revealed that, if ignition occurs, the source is not the burning metal sparks (steel/hard metal), but the transient hot spot generated on the pick after multiple impacts on the rock. In his extensive review paper, Powell (1984) concluded that small burning metal particles from mechanical impacts are not capable of igniting methane/air, and possibly not even higher alkanes/air, unless the particle temperature exceeds 2000°C. This means that steel sparks from single impacts are unlikely to ignite natural gas/air. However, burning particles of titanium, zirconium, magnesium and aluminum can ignite such gases. According to Powell (1984) the low probability of igniting methane/air and group IIA gases/air (see Table 2–2) with steel sparks from single impacts is in accordance with American and British recommendations saying that "non-sparking" tools are superfluous in areas where such gases may be present.

Pedersen and Eckhoff (1986) studied the ignition of propane/air and acetylene/air by heat generated in tangential impacts between tips of different steel qualities or of titanium and a rusty or sandblasted steel plate. Tangential impacts against the steel plate were generated by a rigid spring-loaded arm carrying the test tip. The apparatus is illustrated in Figure 2–20.

The strength of the impact (net impact energy) was expressed in terms of the loss of kinetic energy of the impacting arm during the impact. Some results are shown in Table 2–9.

Within the experimental range of net impact energies up to 20 J, it was not possible to ignite 4.6 vol.% propane/air with sparks or hot spots from single impacts between different steel qualities and rusty or sandblasted steel. This agrees with the general conclusion of Powell (1984) on ignition of groups I and IIA gases, mentioned above.

Table 2–9 Results from Impact Ignition Experiments Using Different Tip Materials Impacting on a Target of Naturally Rusted Steel in an Explosive Mixture of 4.6 vol.% Propane in Air[a]

Tip material	Number of visible sparks	Net impact energy (J)	Ignition
St 37 steel	20–50	8–10	No
Chrome–vanadium steel	10–30	6	No
Unbraco screw	~20	8	No
Acid-resistant screw	~5	8	No
Non-sparking tool	0	13–14	No
Titanium	10–1000	~10–15	Yes

a. *Source*: Data from G. H. Pedersen and R. K. Eckhoff, *Initiation of Gas Explosions by Heat Generated During Single Impact Between Solid Bodies,* CMI Report No. 863302-1, December 1986, Christian Michelsen Institute (now GexCon AS), Bergen. Norway (1986).

However, as Table 2–9 shows, titanium sparks were able to ignite propane/air. In about half of the experiments with titanium that gave ignition, one or several specific flying sparks could be identified by high-speed video as the ignition source(s). Such ignition mostly took place 50–90 ms after the impact. By this time, the velocity of the sparks had dropped to 2–5 m/s, which presumably allowed a sufficient residence time in a given gas volume for ignition to occur. In some cases, single-spark ignition took place after the spark had collided with the wall of the explosion chamber and lost most of its velocity. Similar observations were made by Ritter (1984).

Figure 2–21 shows some more detailed results from impacts with titanium against rust in 4.6 vol.% propane in air. Observe that there seems to be a worst-case range of tangential impact velocities that favors ignition. At lower velocities fewer burning metal particles are produced, and ignition is less probable. At higher velocities more burning metal particles may be produced, but this is more than compensated for by the violent disturbance of the local gas cloud by the movement of the impact arm, which makes ignition less probable.

Some results from ignition of acetylene/air by burning metal particles are given in Table 2–10, showing that highly sensitive gas mixtures can be ignited even if the particle material is stainless steel.

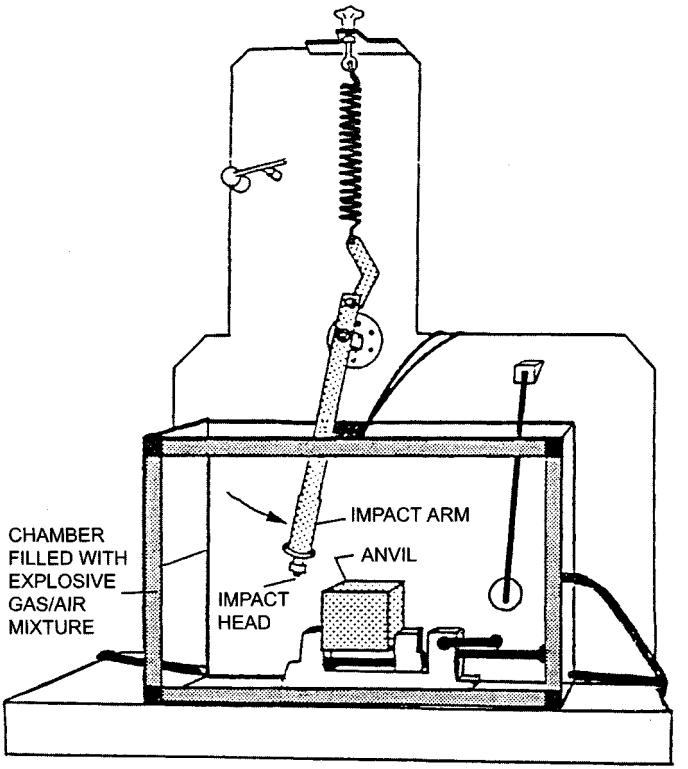

Figure 2–20 Impact spark ignition apparatus used by Pedersen and Eckhoff (1986) for studying the ability of burning metal particles and "thermite flashes" from single impacts to ignite explosive gas/air mixtures.

As can be seen, the acetylene/air mixture was readily ignited by sparks from steel qualities that are known to be less able to release incendiary sparks than standard construction steels. High-speed video recordings revealed that ignition was caused by single flying steel sparks in all the cases covered by Table 2–10. Ignition occurred after the sparks had traveled sufficiently far for the spark velocity to become < 5 m/s. Ignition of acetylene/air by the hot spot generated at the point of impact on the anvil plate was not observed in these experiments.

When using a non-sparking material as the test object, only one single visible spark was observed altogether. This spark became visible 45 ms after the impact, and remained visible for 90 ms. During this period, the spark velocity decreased from about 1 m/s to 0.4 m/s. It is not clear whether this weak spark originated from the non-sparking material or

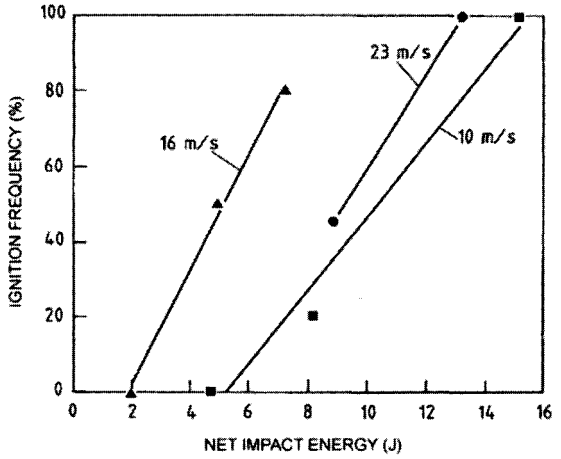

Figure 2–21 Results from tangential impact experiments with titanium against rust in a mixture of 4.6 vol.% propane in air, using the apparatus illustrated in Figure 2–20. From Pedersen and Eckhoff (1986).

Table 2–10 Results from Impact Ignition Experiments Using Different Tip Materials Impacting on a Target of Naturally Rusted Steel in an Explosive Mixture of 7.7 Vol.% Acetylene in Air[a]

Tip material	Number of visible sparks	Net impact energy (J)	Ignition
Chrome–vanadium steel	~10	~6	Yes
Unbraco screw (stainless)	~20	~8	Yes
Acid-resistant steel	3–5	~8	No
Non-sparking tool alloy	0–1	8–10	No

a. *Source*: Data from G. H. Pedersen and R. K. Eckhoff, *Initiation of Gas Explosions by Heat Generated During Single Impact Between Solid Bodies,* CMI Report No. 863302-1, December 1986, Christian Michelsen Institute (now GexCon AS), Bergen. Norway (1986).

from the anvil material, which was rusty steel. Although the spark observed was very weak, its occurrence indicates that impacts involving so-called non-sparking materials as one of the colliding partners may in fact generate visible sparks. However, in view of what has been said above, it seems highly unlikely that such sparks can ignite alkane/air mix-

tures. It is not clear whether impacts between a non-sparking material and light metals, e.g. titanium, may produce incendiary light-metal sparks.

2.2.5.3 Ignition by Thermite Flashes

The experiments in propane/air with impacts of titanium on rusty St37 steel (see Table 2–9) revealed two different modes of ignition. In about half of the tests where ignition occurred, it was observed to take place at or very close to the point of impact on the anvil plate, immediately after or even during impact. In such cases, an extremely luminous hemispherical volume was observed in the region of impact. The onset of flame propagation could neither be referred specifically to one single metal spark nor to the hot spots generated at the points of impact. It is not fully clear what this luminous hemisphere consisted of, but the very high numbers of sparks (of the order of 1,000) that were observed in these cases were located within this volume. The luminous hemisphere was only observed when the peripheral velocity of the tip holder exceeded about 15 m/s. It is believed that the luminous volume was a "thermite flash" corresponding to the overall formal exothermic reaction

$$3Ti + 2Fe_2O_3 \rightarrow 3TiO_2 + 4Fe + \text{heat}$$

Similar reactions would be expected between rust and other metals having greater affinities for oxygen than iron. In the case of aluminum, the softness of the metal may prevent sufficient heat generation during impact to produce a thermite flash. However, according to Kornai et al. (1994), impacts involving harder aluminum alloys may generate thermite flashes, as well as incendiary metal particles. Also, impacts on rusty surfaces covered by aluminum paint of high pigment content have generated thermite flashes. Gibson et al. (1968) demonstrated that smears of aluminum on rusty steel produced thermite flashes capable of igniting methane/air when struck by strikers made from almost any metal, including steel, brass, bronze, and even copper-beryllium.

2.2.5.4 Ignition by Transient Hot Spots

As already pointed out, impacts not only create burning metal particles or thermite flashes but also create transient hot surfaces (hot spots) on the two colliding bodies. Powell and Quince (1972) applied the classical theory of frictional impacts to calculate the maximum hot spot temperatures generated in such impacts. Eckhoff and Pedersen (1988) discussed this theory in relation to impact ignition hazards on offshore oil and gas installations. Cutler (1974, 1978) conducted experiments where methane/air and propane/air were ignited by artificial transient hot spots generated electrically on tungsten strips. Figure 2–22 shows how the values of T_{min} were influenced by the strip width.

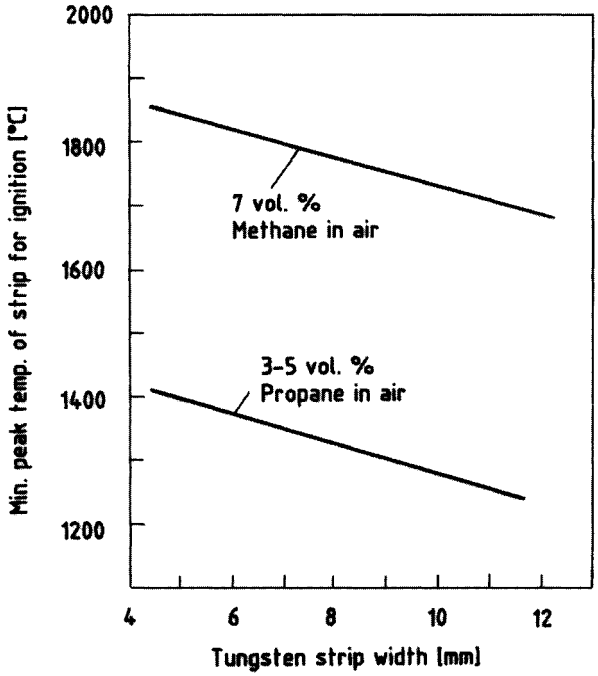

Figure 2–22 Influence of the width of a transiently heated tungsten strip on the minimum peak temperature of the strip for igniting methane/air and propane/air. Data from Cutler (1974, 1978).

As pointed out above, experiments with net impact energies of up to 20 J in acetylene/air revealed that ignition never occurred at the hot spot on the anvil plate or on the impacting metal tip. Therefore, net impact energies that are substantially higher than 20 J would be required for generation of hot spots by single impacts, which would be capable of igniting natural gas/air.

2.2.6 Ignition by Electric Sparks and Arcs and Electrostatic Discharges

2.2.6.1 Electric Sparks between Two Conducting Electrodes

Electric sparks are produced when the strength of the electric field in the gap between two conducting electrodes exceeds what the dielectric medium in the gap can resist. For a given dielectric medium, e.g. air at atmospheric conditions, the relationship between the gap distance and the critical gap voltage for gap breakdown depends on the electrode shape and the electrode material.

Figure 2–23 gives some results obtained in two different laboratories from measurement of electrical breakdown voltages in air at atmospheric conditions using various electrode configurations. All data confirm that, for one specific electrode system, the electrical breakdown voltage increases systematically with the length of the gap between the electrodes. Also, the data confirm that for a given gap length the electrical breakdown voltage is considerably lower with needle point electrodes than with rounded electrodes having radii of curvature of at least a few mm. The discrepancies between the absolute breakdown voltages obtained in the two laboratories for apparently similar conditions illustrate that the actual breakdown voltage also depends on other experimental conditions than just global electrode shape and gap distance.

Extrapolation of the various curves in Figure 2–23 into the region of voltages of the order of 100 V and less indicate that spark-over will then be possible only at very small gap distances $<<$ 1 mm. This in turn means that any ignition of an explosive gas mixture under such circumstances occurs under partly quenched conditions (see Figure 2–26). This means that the required spark energy for ignition can be considerably higher than the minimum ignition energies obtained under unquenched conditions.

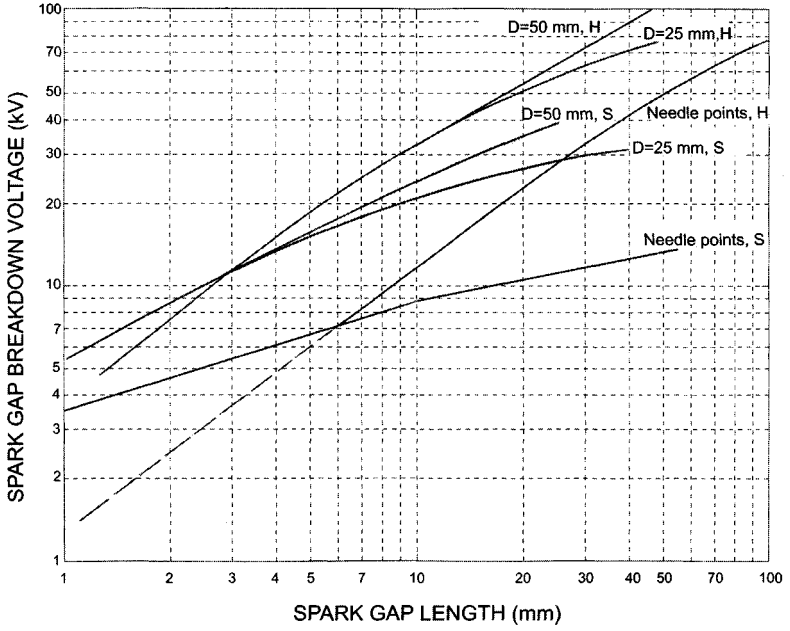

Figure 2–23 Spark gap breakdown voltages in air at normal atmospheric conditions as functions of spark gap length and electrode shape. "H" indicates data from Handbook of Chemistry and Physics (1959/60) and "S" indicates data from Smithsonian Physical Tables (1959). Details of electrode materials and electrode surface structures are not known.

Electric sparks can be capacitive, inductive, or resistive. Capacitive sparks, associated with the discharge of a capacitor across a given spark gap, can occur in electric circuits, or they can be caused by tribo-electrically generated electrostatic charges. The theoretical spark energy, neglecting losses, is $\frac{1}{2}CV^2$, where C is the capacitance and V is the voltage across the spark gap just prior to gap breakdown. Inductive sparks are associated with discharge of inductive energy across gaps that are formed when live circuits are broken. In this case, the theoretical spark energy is $\frac{1}{2}Li^2$ where L is the inductance and i is the current just before formation of the break. Any given explosive mixture of a combustible gas and air is associated with a given minimum value of electric spark energies E_{min} that can ignite the mixture. Figure 2–24 illustrates this for the alkanes, e.g. which constitute the main components in natural gas from the North Sea. It is seen that the values of the equivalence ratio Φ at which the minimum ignition energy for each gas occurs increase systematically

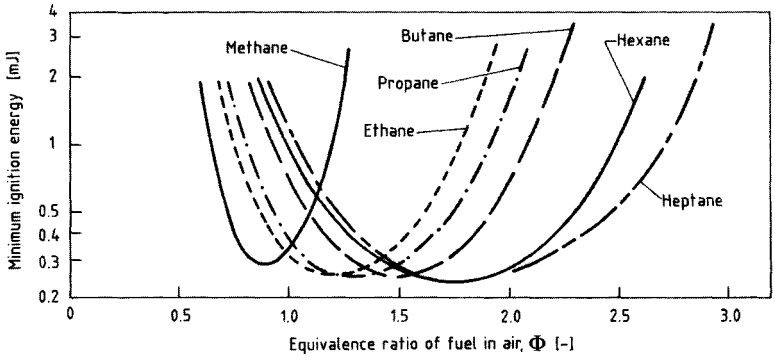

Figure 2–24 Minimum capactive electrical spark ignition energies of mixtures of various gaseous alkanes and air as a function of the volumetric ratio of fuel and air. For $\Phi = 1$ the ratio of fuel to oxygen is stoichiometric. For $\Phi < 1$ the mixture is lean and for $\Phi > 1$ it is rich.

with increasing molecular weight of the fuel gas, from 0.85 for methane (Mw = 16) to 1.80 for heptane (Mw = 100). It is also seen that the standard E_{min} value of methane (0.28 mJ) is slightly higher than those of the higher alkanes (0.23–0.25 mJ).

Figure 2–25 shows curves corresponding to those in Figure 2–24, for a range of different explosive gas/air mixtures. As can be seen, E_{min} for the most ignition sensitive gases hydrogen, acetylene and carbon di-sulphide, are about two orders of magnitude lower than the values for the alkanes in Figure 2–24.

All the E_{min} values in Figure 2–24 and Figure 2–25 were determined by capacitive sparks under unquenched conditions, which implies that the fixed spark gaps used in the test were slightly larger than the quenching distances QD for the gas mixtures tested. This quenching distance concept is illustrated in Figure 2–26. True E_{min} values are obtained only if the length of the electrode gap exceeds QD. As soon as the gap length becomes < QD the minimum spark energy for ignition can increase quite significantly. The increase will be more or less abrupt, depending on the physical dimensions of the electrodes, as illustrated in Figure 2–26.

Figure 2–27 illustrates the close correlation between E_{min} and QD.

It is generally assumed that the minimum ignition energies obtained for capacitive sparks by optimizing spark gap length and fuel/air ratio are the true minima. However, this may not be entirely true. Figure 2–28 gives

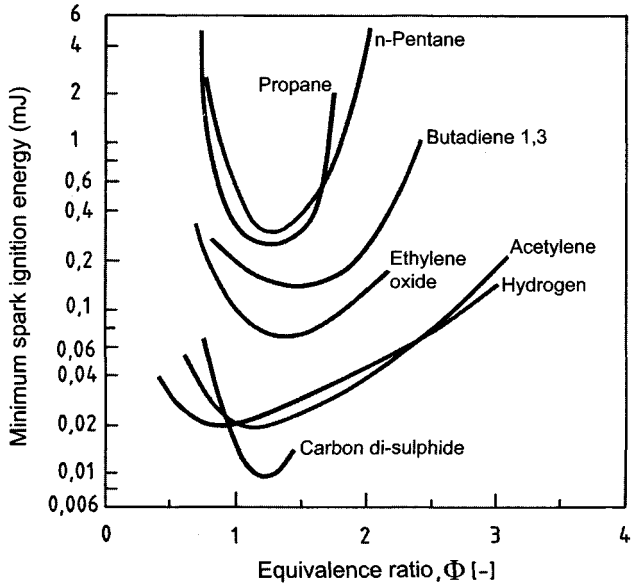

Figure 2–25 Minimum capacitive electrical spark ignition energies of mixtures of various gaseous fuels and air as a function of the volumetric ratio of fuel and air. For $\Phi = 1$ the ratio of fuel to oxygen is stoichiometric. For $\Phi < 1$ the mixture is lean and for $\Phi > 1$ it is rich.

some results from a study by Parker (1985), showing that minimum ignition energies may also depend on the basic features of the spark discharge. Using constant-power sparks of mutually independent energy and duration, Parker found that the minimum ignition energy of a lean propane/air mixture increased from about 0.2 mJ for 0.1 μs discharge duration to about 2 mJ for 100 μs duration. The reason for this quite pronounced effect may be found in the fundamental process of ignition, where the production of chemically active radicals in the spark, which is enhanced by the high spark temperatures generated at short discharge times, plays a central role.

Various electrical apparatus can give rise to electric sparks and arcs that can cause ignition of explosive gas mixtures. Electric sparks can be generated when electric circuits are opened and closed, or by stray currents. The use of low-voltage equipment (maximum = 50 V) for protecting personnel against electric shock does not eliminate the explosion hazard. Even lower voltages than this can produce energies which can ignite explosive gases. It has been found useful, therefore, to introduce an

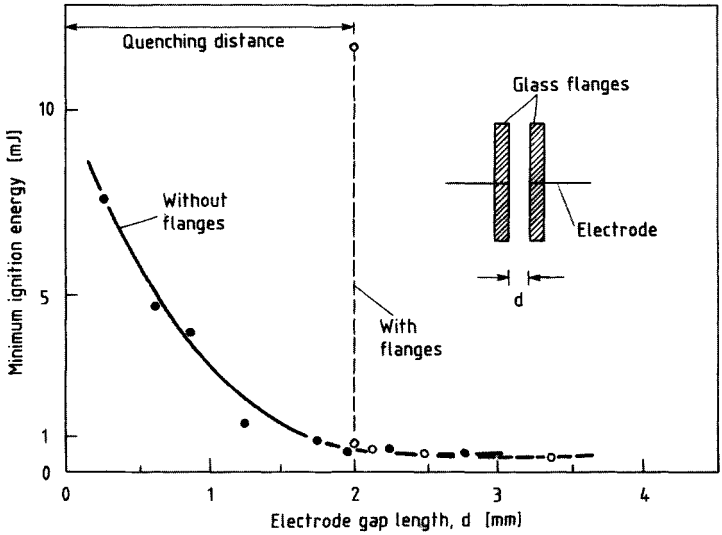

Figure 2–26 Minimum capacitive electric spark energies for ignition of a stoichiometric mixture of natural gas and air, as a function of length of gap between electrodes, with and without glass flanges at the electrode tips. Data from Freytag (1965).

international standard method for experimental determination of the combinations of electrical circuit parameters that are critical for producing incendiary sparks/arcs from electrical circuitry. The IEC standard apparatus is illustrated in Figure 2–29.

Figure 2–30 shows experimental ignition curves (solid lines) for propane/air (IIA), ethylene/air (IIB) and hydrogen/air (IIC) determined in the apparatus illustrated in Figure 2–29. Ignition occurred at capacitor voltages even below 10 V, which is only possible with minute spark gap lengths of << 1mm. This in turn means that the sparks were delivered to the explosive mixture under quenched conditions (see Figure 2–26). It is not surprising, therefore, that the dotted lines, representing the minimum $\frac{1}{2}CU^2$ for igniting the three different gas mixtures with spark gaps > the quenching distances, falls significantly below the experimental solid lines.

As shown in Figure 2–31, a corresponding effect is found for inductive circuits, where the lines for $\frac{1}{2}Li^2 = E_{min}$ are also significantly below the corresponding minimum break flash ignition curves (minimum ignition current as a function of circuit inductance).

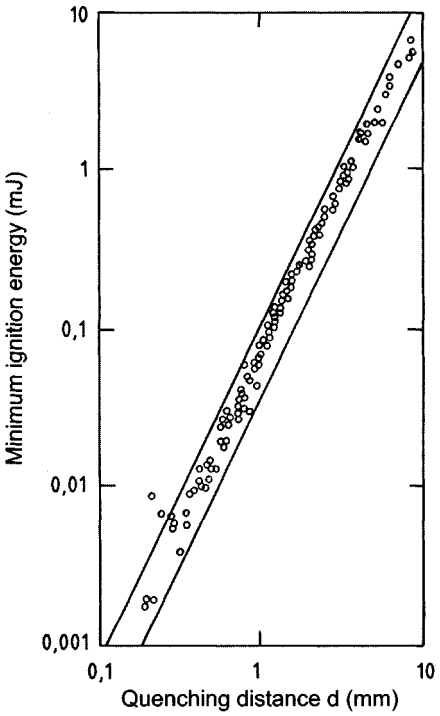

Figure 2–27 Correlation of minimum electric spark ignition energies for unquenched ignitions, and corresponding quenching distances. From Kuchta (1985).

Besides sparks from electrical apparatuses, spark discharges between two conducting electrodes can also arise from tribo-electric charging of non-earthed electrically conducting items. Table 2–11 indicates the levels of capacitance C and voltage V that may be associated with electrostatic charging of non-earthed electrical components in industry. The resulting stored energies $\frac{1}{2}CV^2$ represent the maximum spark energies that can be generated from discharge of the various capacitive components to earth.

Table 2–11 also includes the charging of a human being. For example, charging can occur whenever a person wearing electrically insulating shoes is walking across a floor. Charge transfer occurs every time the shoes are lifted or separated from the floor. Figure 2–32 illustrates the discharge of an electrostatically charged person to earth. In electrical terms, the human body can be regarded as a capacitor of the order of 100–300 pF, with a given internal ohmic resistance. It is commonly

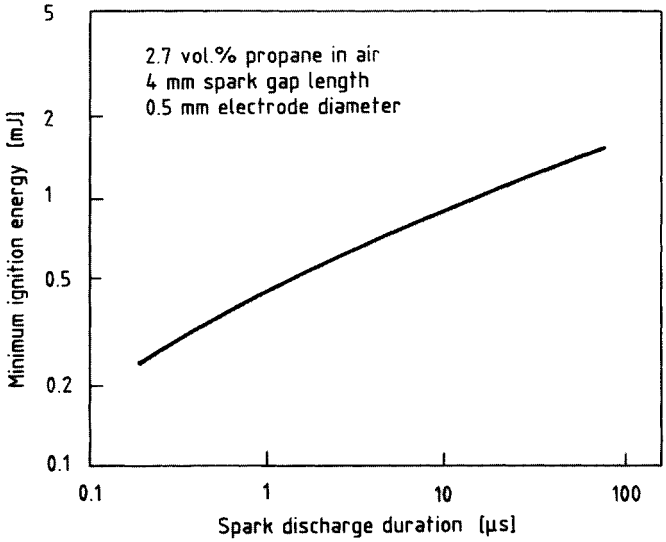

Figure 2–28 Influence of spark discharge duration on minimum ignition energy of a lean (2.7 vol.%) mixture of propane/air at normal temperature and pressure. Data from Parker (1985).

assumed that during discharge about half the energy $\frac{1}{2}CV^2$ stored in the capacitor is dissipated in the spark and the other half in the internal body resistance. As Table 2–11 shows, spark energies well above E_{min} for most gases and vapors can be generated when a charged person is discharged to earth. In many process operations it is therefore necessary to take active measures to make sure that electrostatic charging of persons cannot occur, or to ensure that any charged person is reliably discharged before entering an area where explosive gas atmospheres may occur.

The most important measure for preventing electrostatic spark discharges is earthing of all conductive parts that could become dangerously charged (see Table 2–11). However, this protective measure is insufficient if non-conductive materials are present and become electrostatically charged to hazardous levels. In this case electrostatic one-electrode discharges can occur which may also ignite explosive gas/air mixtures. Then non-conductive materials must be avoided. This may imply that only earthed metals and earthed anti-static non-metals are permissible in e.g. process equipment.

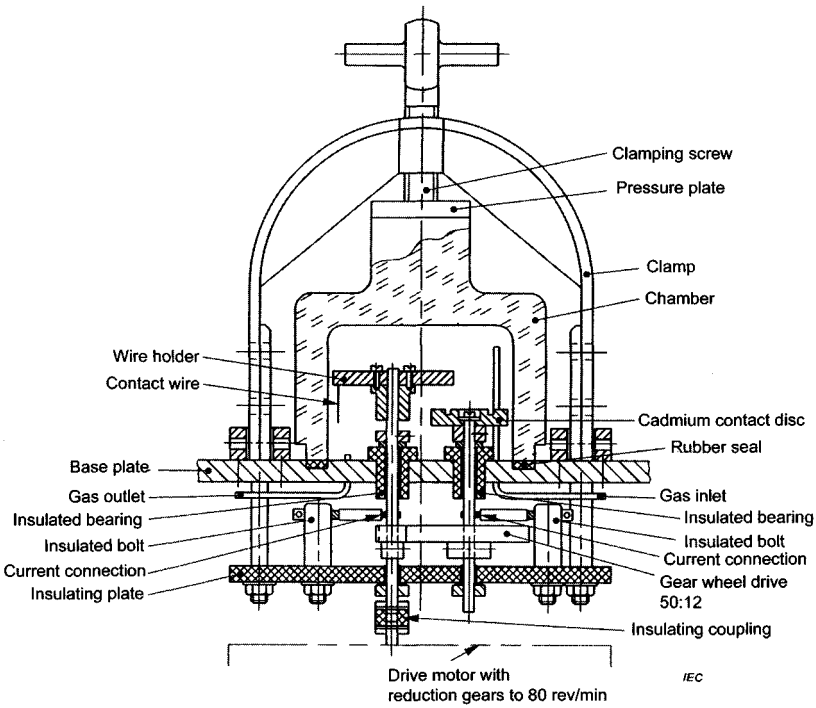

Figure 2–29 Standardized IEC apparatus for experimental determination of ignition curves, and for testing of the ability of electrical circuits to produce sparks that can ignite gas mixtures. From IEC (1999).

2.2.6.2 Various Forms of One-Electrode Electrostatic Discharges from Charged Non-Conductors: Concept of "Equivalent Energy"

A one-electrode discharge occurs when electrostatic charge accumulated on the surface of a non-conductor by a charge separation process, is drained to earth via a conducting electrode approaching the charged non-conductor. It is common to distinguish between three types of one-electrode discharges

(1) corona discharge

(2) brush discharge

(3) propagating brush discharge

Lüttgens and Glor (1989) and Lüttgens and Wilson (1997) have discussed the nature of the three types of discharges in detail and have illustrated their possible appearance in practice by examples.

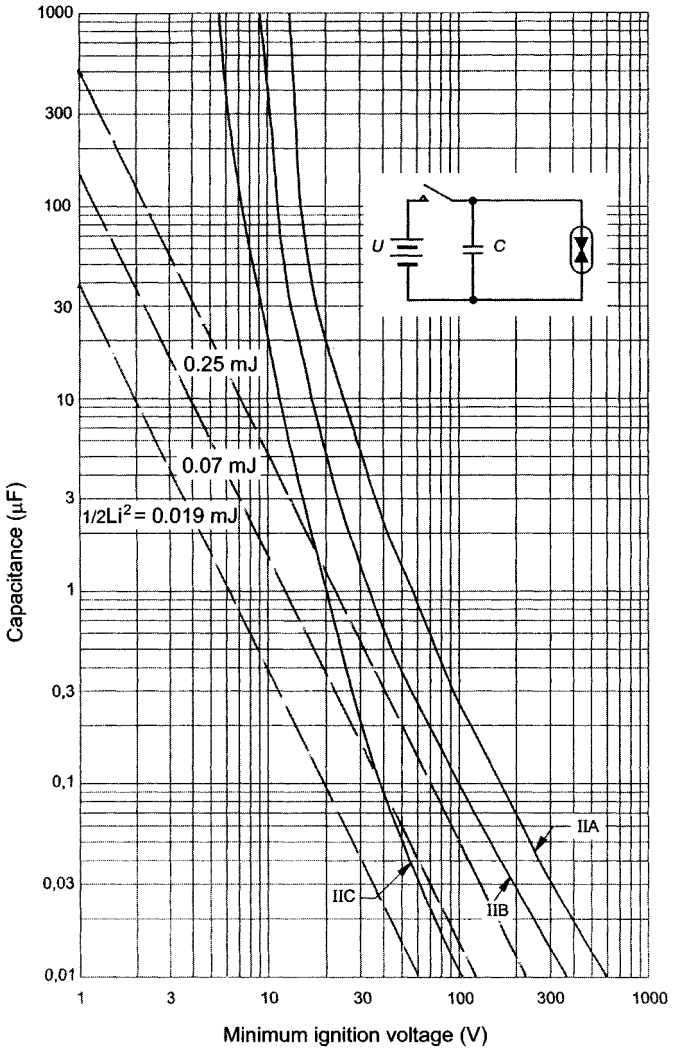

Figure 2–30 Experimental standard ignition curves for propane/air (IIA), ethylene/air (IIB) and hydrogen/air (IIC) for capacitive spark discharges, determined by the standard IEC break flash apparatus shown in Figure 2–29. The dotted straight lines represent all combinations of voltage and capacitance that yield ½ CU^2 values equal to the experimental minimum ignition energies for the three respective gas mixtures. The standard ignition curves are taken from IEC (1999).

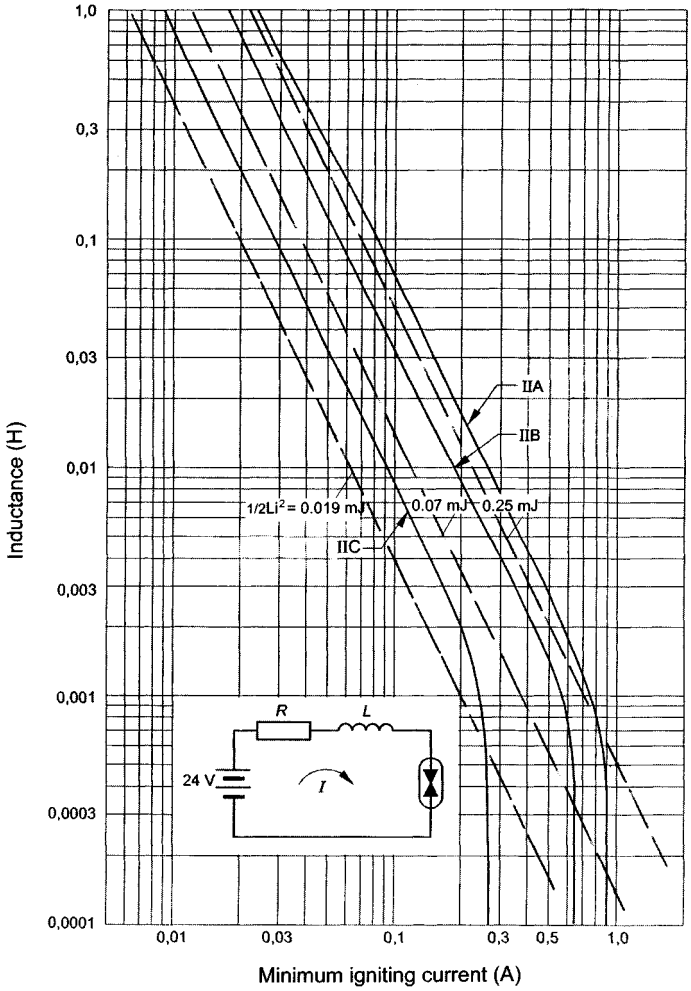

Figure 2–31 Experimental standard ignition curves for propane/air (IIA), ethylene/air (IIB) and hydrogen/air (IIC) for inductive spark discharges, determined by the standard IEC break flash apparatus shown in Figure 2–29. The dotted straight lines represent all combinations of current and inductance that yield ½ Li^2 values equal to the experimental minimum ignition energies for the three respective gas mixtures. The standard ignition curves are taken from IEC (1999).

Corona discharges, illustrated in Figure 2–33, occur when the tip of a pointed conducting electrode (radius of curvature < 1 mm) approaches a charged non-conductor. This type of discharge does not occur abruptly

Table 2-11 Examples of Combinations of Capacitances and Voltages and Resulting Spark Energies in Industrial Practice

Charged object	Capacitance (pF)	Potential (kV)	Energy (mJ)*
Single screw	1	5	0.01
Flange, nominal width = 100 mm	10	10	0.5
Shovel	20	15	2
Small container (~50 litres)	50	8	2
Funnel	50	15	6
Person	300	10	15
Drum (200 litres)	200	20	40
Road tanker	1000	15	100

Data are taken from Luttgens and Glor (1989)
*Approximate values

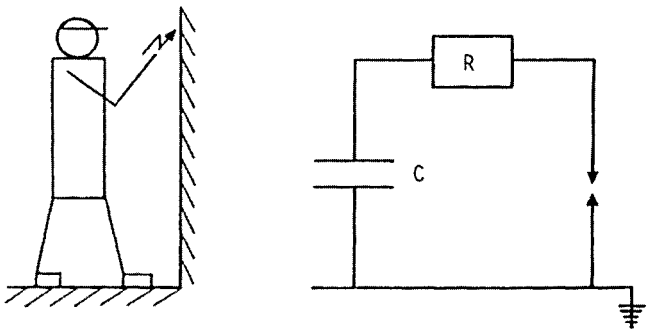

Figure 2–32 Discharge of an electrostatically charged person to earth. Approximate equivalent electrical circuit of a human being, with internal resistance and capacitance in series. From Glor (1988).

within a short time interval as a spark, but rather as a continuous charge leakage, and only gas mixtures of very low minimum ignition energies can be ignited by corona discharges.

However, when the radius of curvature of the conducting electrode tip exceeds a few min, the discharge will occur more abruptly, and a stem of high energy density will appear close to the electrode. Because of this appearance, this type of discharge, illustrated in Figure 2–34, is called a *brush discharge.*

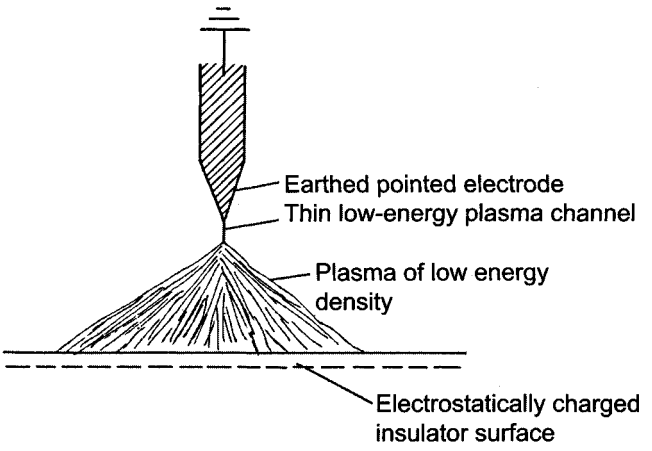

Figure 2–33 Illustration of a corona discharge from a charged insulator surface to earth.

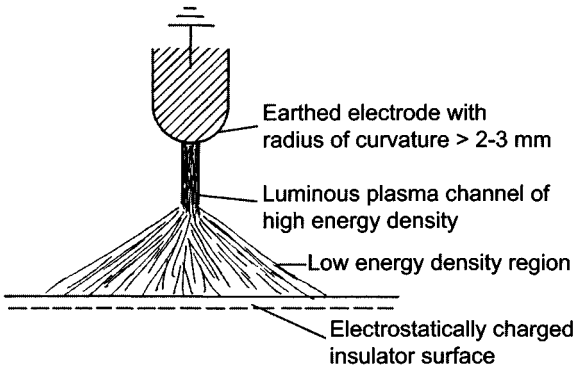

Figure 2–34 Illustration of a brush discharge from a charged insulator surface to earth.

Substantially stronger and more incendiary *propagating brush discharges* than ordinary brush discharges can be obtained if a charged double layer of opposite polarities is generated rather than just a single charge layer, as illustrated in Figure 2–35 and Figure 2–36. This can occur if an insulating film is charged tribo-electrically with opposite charge polarity on both sides, or if the side of the film which is not charged directly can be charged by induction from a distant or close earthed object.

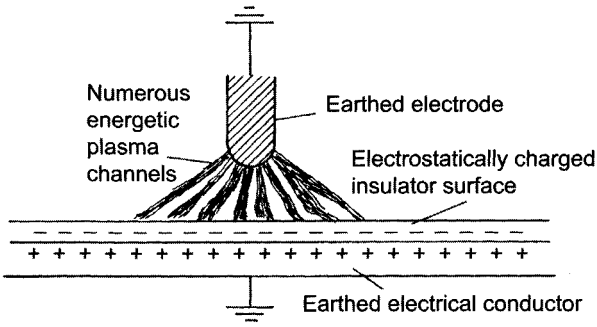

Figure 2–35 Illustration of a propagating brush discharge occurring when an earthed electrode is brought close to the charged insulator surface that is in contact with an earthed conductor.

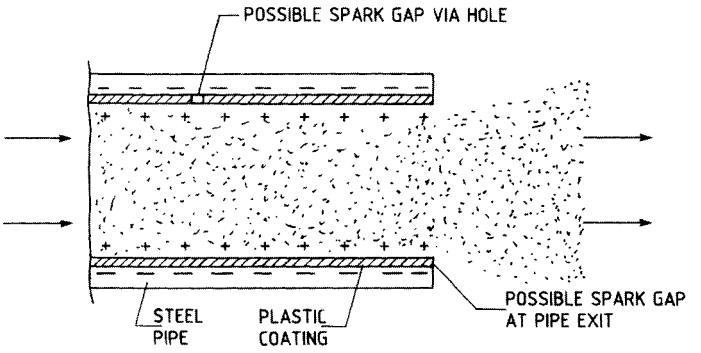

Figure 2–36 Illustration of a propagating brush discharge occurring in a steel pipe lined with an insulating film, when the strong electric field breaks down the charged insulating film and drains the charge to earth through the breakdown channel. Alternatively the charge can occur across a gap at the pipe exit.

For basic reasons, the energy of the incendiary part of a corona, brush or propagating brush discharge is not easy to measure directly. The concept of *equivalent energy* is useful in partly overcoming this problem. This concept, which was first introduced by Gibson and Lloyd (1965), is defined as follows: An electric discharge has the equivalent energy W if it is just capable of igniting an explosive mixture of $E_{min} = W$. The equivalent energy of any reproducible but not quantifiable electric discharge is determined in two steps. The first is to determine the composition of a pre-mixed fuel/air/nitrogen mixture, which can just be ignited by the unknown discharge. The second step is to determine E_{min} of that particular mixture, which will per definition be equal to W. The equivalent energies for the three types of one-electrode discharges discussed above are indicated in Table 2–12.

Table 2–12 Equivalent Energies of Three Types of Electrostatic One-Electrode Discharges

Type of discharge	Equivalent energy (mJ)
Corona	$\leqslant 2 \times 10^{-2}$
Brush	$\leqslant 3$
Propagating brush	$\leqslant 10^5$

Data from Lüttgens and Glor (1989)

The minimum ignition energy for alkanes in air is of the order of 0.25 mJ. Therefore, it is unlikely that such mixtures, including natural gas in air, can be ignited by corona discharges. However, brush discharges may cause ignition, and propagating brush discharges can generate energies that are substantially higher by orders of magnitude than those required for ignition.

2.2.7 Ignition by a Jet of Hot Combustion Products

2.2.7.1 The Basic Process

The situation is illustrated in Figure 2–37.

The central question is whether the hot jet will ignite an explosive gas cloud outside the enclosure of the same composition as the one exploding inside. Systematic research has been carried out to investigate the influence on the probability of ignition of hole diameters/slot width, the length

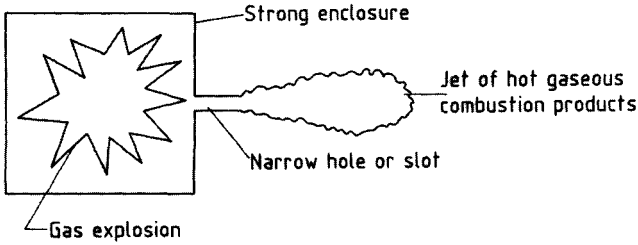

Figure 2–37 Illustration of the ejection of a jet of hot gaseous combustion products through a narrow hole or slit in the wall of a strong enclosure in which a gas explosion takes place.

of hole/slot, the volume of the enclosure in which the primary explosion takes place, the volume of the external explosion chamber, the location of the ignition point inside the primary enclosure, and of course the composition of the gas mixture.

2.2.7.2 Grouping of Ignition Sensitivity of Premixed Gas/Air According to MESG

Various standard test apparatuses (see Figure 2–44) have been designed to determine the maximum experimental safe gap (MESG) for a given explosive gas mixture. Experience has shown that there is a correlation between MESG values obtained in such tests and the quenching distance (QD) discussed above (Figure 2–26). A rough rule of thumb is that QD $\approx 2 \cdot$ MESG. Keeping in mind that there is a strong positive correlation between the quenching distance of a gas mixture and its minimum ignition energy (Figure 2–26), one would expect MESG to vary with gas type and fuel/air ratio in a manner similar to that in Figure 2–24 for the minimum ignition energy. As shown in Figure 2–38, this is indeed the case. Table 2–2 gives some MESG values from standards tests (Figure 2–44) and the resulting grouping of the gases tested in gas groups.

Figure 2–39 shows the apparatus used in some gas explosion transmission experiments conducted by Larsen and Eckhoff (2000). The vertical cylindrical system consisted of two concentric chambers, one primary and one secondary, separated by a disc with the cylindrical transmission hole at its center. Before an experiment both chambers were flushed with premixed propane/air of the desired composition, until this concentration was obtained throughout the system. The electric spark ignition source in the

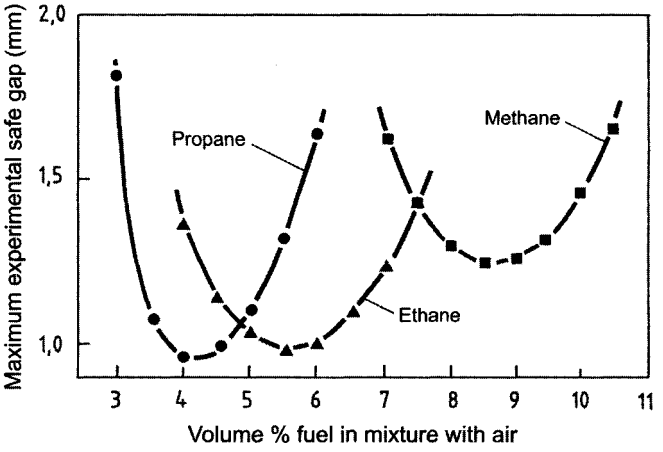

Figure 2–38 Influence of fuel concentration in mixtures with air on MESG for the three lower alkanes. Data from Alfert (1985).

primary chamber was positioned at the chamber axis, and the distance X_i from the ignition point to the entrance of the transmission hole was varied.

Figure 2–40 gives a set of results showing the critical distance X_i for explosion transmission as a function of the hole diameter D. As can be seen, the critical hole diameter for flame transmission with $X_i = 0$ was about 3 mm. In this case the conditions were probably close to laminar, and what was measured was the critical laminar quenching tube diameter.

However, as X_i was gradually increased, a significant amount of gas had to burn before the flame front reached the hole entrance. This means that at the time of flame front arrival at the hole entrance the pressure in the primary chamber was significantly higher than the ambient pressure downstream of the transmission hole. Hence, when the flame front arrived at the hole, hot combustion gases were pushed through the hole, producing a jet into the unburned explosive gas in the secondary chamber. The question was then no longer whether a laminar flame front would be able to travel through the transmission hole, but rather whether re-ignition would occur downstream of the hole, where the hot combustion gases ejected from the hole mixed with the unburned mixture. As Figure 2–40 shows, it appeared that the minimum critical hole diameter for such re-

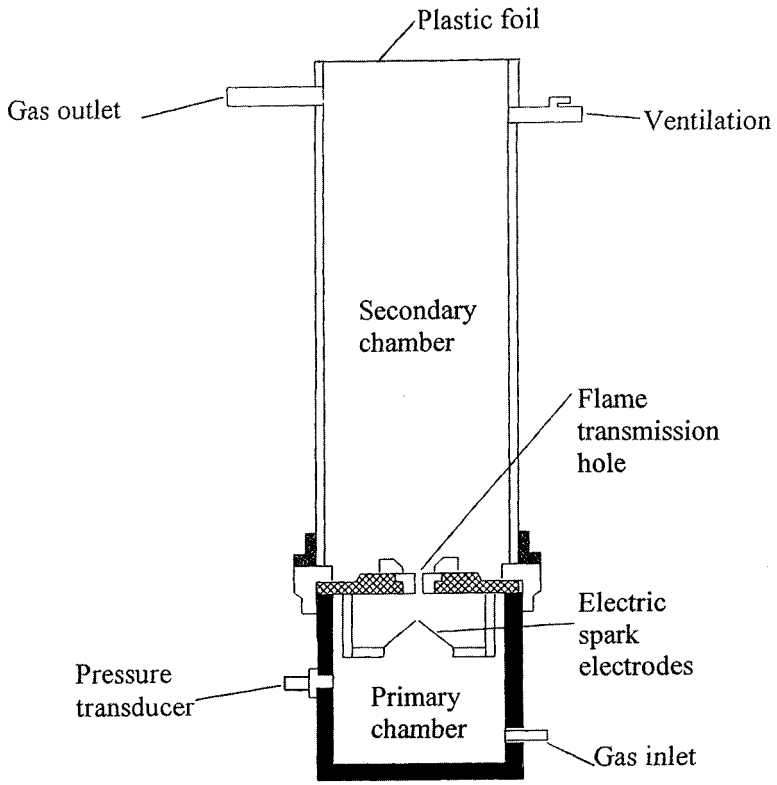

Figure 2–39 Cross section of apparatus used by Larsen and Eckhoff (2000) for experimental determination of critical hole diameters for transmission of gas explosions. The volume of the primary chamber was 1 liter.

ignition was in fact about half the critical diameter in laminar flame transmission. However, with a further increase of X_i the critical hole diameter for re-ignition increased far beyond the laminar flame transmission value. This is because, at large X_i values, the overpressures in the primary chamber reach high values at the moment of flame arrival at the hole entrance, and give rise to correspondingly high jet velocities. This in turn causes very fast mixing of the hot combustion products and the cold unburned mixture, and the whole system cools down before the combustion chemistry gets under way.

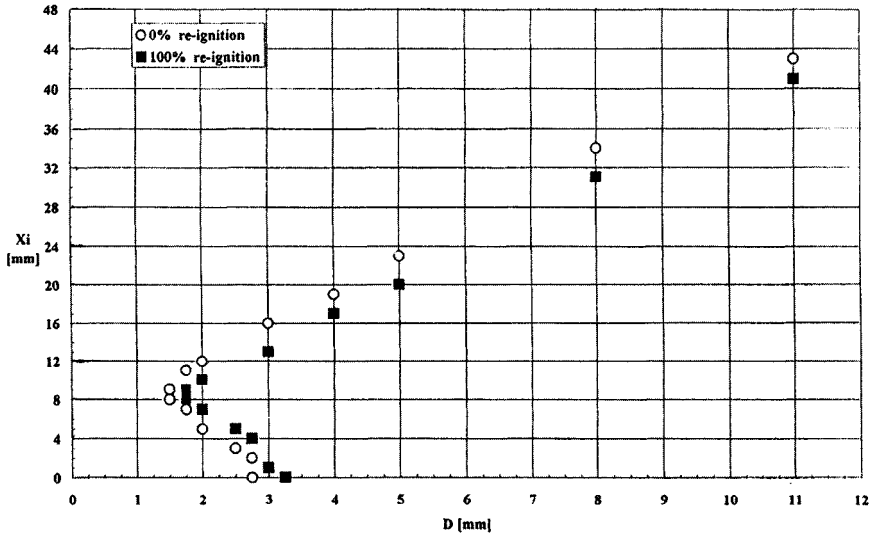

Figure 2–40 Results from experiments with a cylindrical 1 liter primary chamber (Figure 2–39). X_i is the distance from the electric spark ignition source on the chamber axis to the entrance of the axial cylindrical transmission hole of diameter D and length 12.5 mm. Explosive gas mixture: 4.2 vol.% propane in air. From Larsen and Eckhoff (2000).

Figure 2–41 shows two high-speed video pictures at critical conditions for re-ignition, using a smaller primary chamber than that illustrated in Figure 2–39. With X_i = 8 mm re-ignition occurred, with X_i = 9 mm there was no re-ignition. The characteristic difference between the two cases is the flame ball that appears in the downstream region of the jet in the case of re-ignition.

Results from some earlier similar studies by Wolfhard and Bruszak (1960) are given in Figure 2–42. In this case, the gas mixtures in the primary and secondary chambers were different. The gas in the primary chamber was stoichiometric mixtures of methane, oxygen, and nitrogen in all the experiments. The ratio of oxygen to nitrogen was varied and characterized by the oxygen index (OI) = (vol.% O_2)/(vol.O_2 + N_2). The purpose of the experiments was to determine the critical OI in the primary chamber for re-ignition in the secondary chamber. The three fuel gases used in the secondary chamber were methane, ethane and a mixture of 90 vol.% CO and 10 vol.% H_2, and they were mixed with air to stoichiometric compositions. The gap for the electric spark used for igniting the

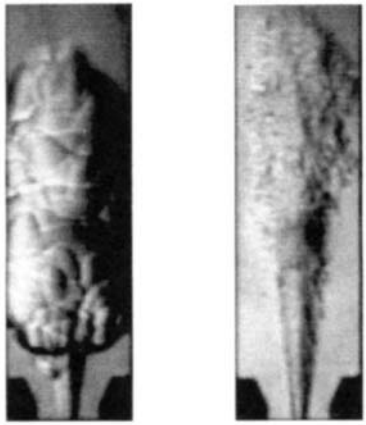

Re-ignition No re-ignition

Figure 2–41 High speed video Schlieren pictures of hot-gas jets expelled from a 0.021 liter primary chamber into a larger secondary chamber via a straight cylindrical hole of diameter 4 mm and length 12.5 mm. 4.2 vol.% propane in air in both primary and secondary chamber. Distance from ignition point in primary chamber to hole entrance was 8 mm for re-ignition and 9 mm for no re-ignition. Pictures taken 6.25 ms after first sign of hot gas jet out of hole. From Larsen (1998).

gas in the primary chamber was located close to the entrance of the tube connecting the two chambers.

As Figure 2–42 shows, the OI required for re-ignition increased systematically with increasing tube length for tube lengths greater than 5–10 mm. The likely reason for this is cooling of the hot combustion gases by the tube wall, which will increase with increasing tube length. For very short tube lengths of a few mm, the critical OI started to rise again. It is also seen that the critical OI for ignition increases with decreasing tube diameter, as would be expected, and with the type of fuel, with methane being the most difficult and CO + H_2 the easiest to re-ignite.

Various apparatuses have been used for determining standardized MESG (maximum experimental safe gap) values of combustible gases and vapors mixed with air (see data in Table 2–2 and Figure 2–44). Normally the primary chamber is spherical, whereas the secondary one is an annulus surrounding the sphere. The connection between the two chambers is a flange gap of length 25 mm and adjustable width. The aim of the test is to determine the critical maximum gap width that does not give re-ignition in the second chamber (MESG), for the actual combustible gas or vapor being tested. The highest values are normally obtained with the

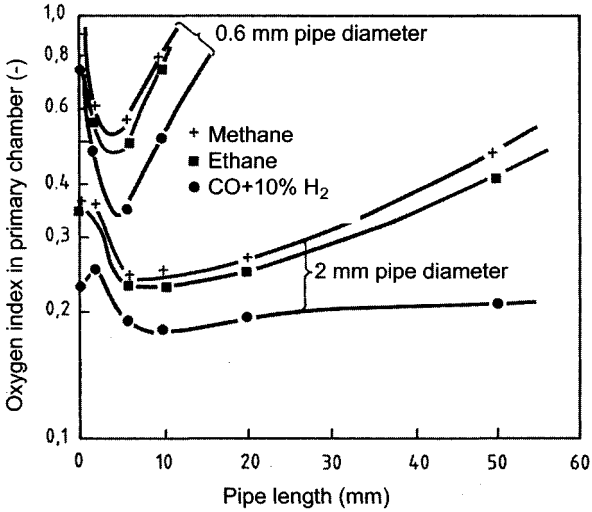

Figure 2–42 Critical oxygen index for ignition of an explosive gas mixture in a secondary chamber by a hot jet of combustion gases from a gas explosion in a primary chamber, as a function of the length of the cylindrical tube connecting the two chambers. Volume of primary chamber: 80 cm^3. Volume of secondary chamber: 3.8 liters. From Wolfhard and Bruszak (1960).

ignition source located fairly close to the gap entrance, rather than at the center of the primary chamber.

Experiments have confirmed that the volume of the primary chamber does not influence the measured MESG as long as this volume is at least 20 cm^3, and the volume of the secondary chamber is sufficiently large to prevent pre-compression of the gas there before the appearance of the hot jet. This is illustrated in Figure 2–43.

As can be seen no significant effect of the volume of the primary chamber was found over the range 0.020–8.0 liters. For this reason it was decided to adopt a primary chamber of 0.020 liter volume in the standard IEC (1971) test method. Figure 2–44 shows the standard apparatus developed by IEC (1975a). Prior to an experiment the width of the 25 mm long flanged gap is adjusted to the desired value by means of a spring-loaded micrometer screw. The ignition source in the internal chamber is a 3 mm spark gap located perpendicularly to the gap plane, 14 mm away from the gap entrance. The chambers are flushed with the gas/air mixture to be tested until homogeneous composition is obtained throughout. Whether re-ignition occurs is observed visually through the glass window in the

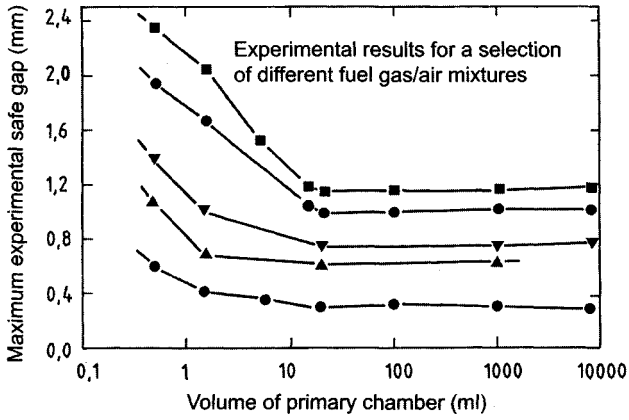

Figure 2–43 Influence of the volume of the primary chamber on MESG, determined experimentally by PTB, Germany. From Phillips (1987).

wall of the external chamber. The MESG data in Table 2–2 were determined by this method.

Figure 2–45 gives some experimental results from Maskow (1950) showing the effect on MESG of varying both the length of the gap from the standard 25 mm and downwards, and the fuel/air ratio.

This figure shows that the critical gap width for flame transmission (re-ignition downstream of gap) increased systematically with the gap length L, apart from a sharp edge (L = 0) being slightly less efficient than a short finite gap of length 1 mm. It is also seen that the fuel/air ratios that gave flame transmission most readily were close to the stoichiometric ratio.

2.2.8 Ignition by Rapid Adiabatic Compression

In the case of rapid adiabatic compression, much work has been performed in the context of internal combustion and diesel engines. Some useful information is given in Freytag (1965). If an explosive gas mixture is compressed rapidly adiabatically, or in a shock wave, the temperature will rise rapidly and the cloud may ignite. The temperature increase mainly depends on the ratio between the pressure after compression and the initial pressure. Shock waves may be generated during sudden relief

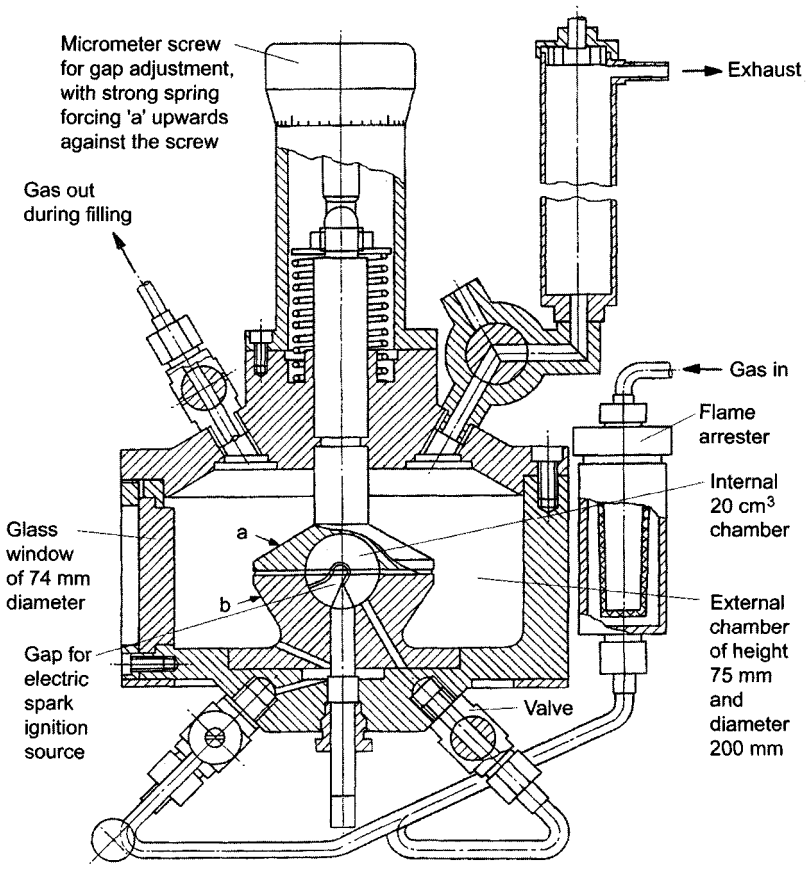

Figure 2–44 Illustration of the standard IEC apparatus used for determination of MESG for combustible gases and vapors mixed with air. Volume of primary spherical chamber is 20 cm^3. Standard gap length 25 mm. From IEC (1975a).

of high-pressure gases into pipelines. The shock wave then propagates into regions of lower pressure faster than the speed of sound. Very high peak pressures and temperatures can occur if the wave is diffracted or reflected by pipe bends, constrictions, connection flanges, closed valves etc.

Figure 2–46 shows pressure as a function of time during rapid compression of a mixture of hydrogen and air in a cylinder with a piston. The induction time between completion of compression and onset of ignition is a characteristic feature of this kind of process. Figure 2–47 and

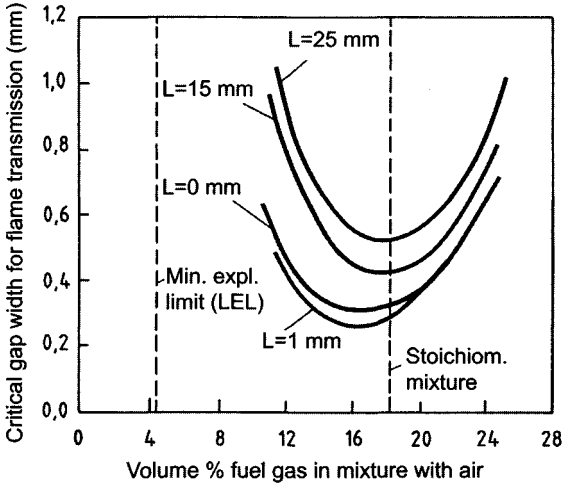

Figure 2–45 Maximum experimental safe gap, determined in a standard MESG test apparatus, for different gap lengths L and different fuel/air ratios. Fuel: 30 vol.% methane + 70 vol.% hydrogen. From Maskow (1950).

Figure 2–48 show experimental results for some hydrocarbons. The induction time depends both on the fuel type and the fuel/air ratio, and on the degree of compression (temperature of gas mixture just after compression has been completed). Fuel/air ratios of about half the stoichiometric composition seem to ignite most easily in this ignition mode.

A more recent, detailed study of ignition following rapid adiabatic compression of heptane/air mixtures, was undertaken by Minetti et al. (1995).

2.2.9 Ignition by Light Radiation

Some informative investigations were conducted by Welzel et al. (2000) and Thowle (2000). Welzel et al. studied ignition of a wide range of explosive gases and vapors mixed with air, by continuous optical radiation conveyed through an optical fiber and absorbed by a solid black iron/manganese oxide target mounted at the end of the fiber. The combustible gases and vapors covered a wide range of auto-ignition temperatures The experimental apparatus used is illustrated in Figure 2–49.

The ignition chamber containing the explosive gas mixture was a vertical glass tube of length 50 cm and diameter 15 cm, i.e. a volume of about 9 liters. The iron-oxide-covered end of the optical fiber was positioned in

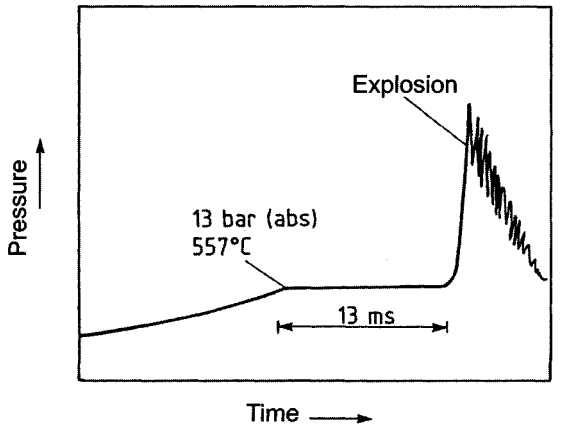

Figure 2–46 Pressure as a function of time during rapid compression of a mixture of hydrogen and air in a cylinder with piston. State of gas mixture at end of compression: 13 bar (abs) and 557°C. Induction time 13 ms. From Freytag (1965).

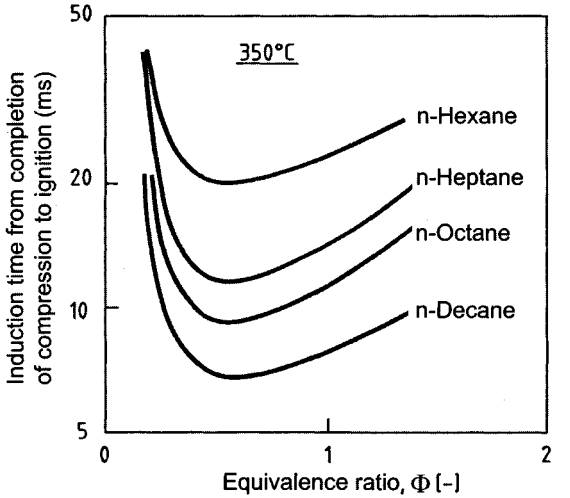

Figure 2–47 Induction time as a function of fuel/air ratio for some alkane/air mixtures compressed adiabatically to 350°C. (Φ = 1 corresponds to the stoichiometric ratio). From Freytag (1965).

the lower part of the chamber. The light source was a laser of wavelength 1064 nm. Figure 2–50 shows a selection of experimental results. The Figure also indicates conservative limits embracing all the data, viz.

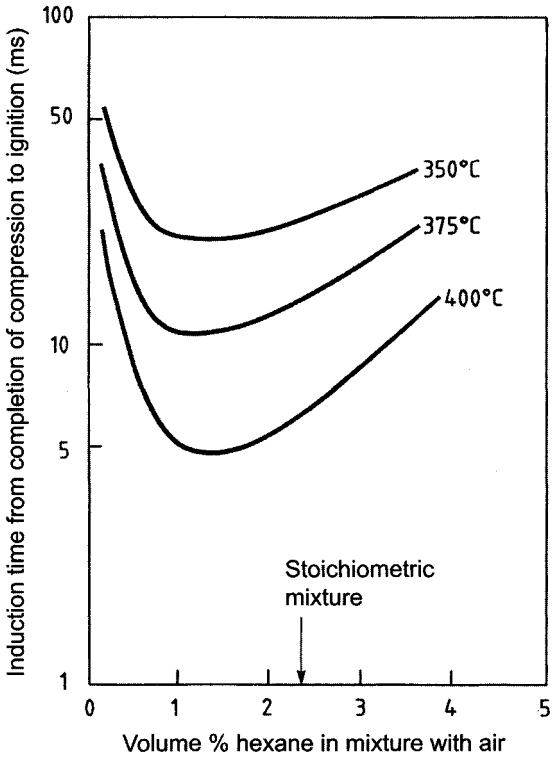

Figure 2–48 Induction time as a function of fuel/air ratio for hexane/air for various degrees of adiabatic compression. From Freytag (1965).

35 mW for target areas smaller than 4 mm^2, and 5 mW/mm^2 for larger target areas.

Figure 2–51 illustrates how the minimum radiant power required for ignition drops with increasing temperature of the explosive mixture.

Figure 2–52, from Thowle (2000), summarizes data from several independent investigations, including that of Welzel et al. (2000), and the data confirm the validity of the conservative asymptotes suggested by Welzel et al (2000). Note that the very low values in the lower right corner of Figure 2–52 were obtained by targets heated electrically, not by light radiation.

Correspondence of the absorption bands of the combustible gas with the laser or radioactive radiation wavelength may cause ignition by direct excitation and ionization of the gas molecules. Radioactive radiation is

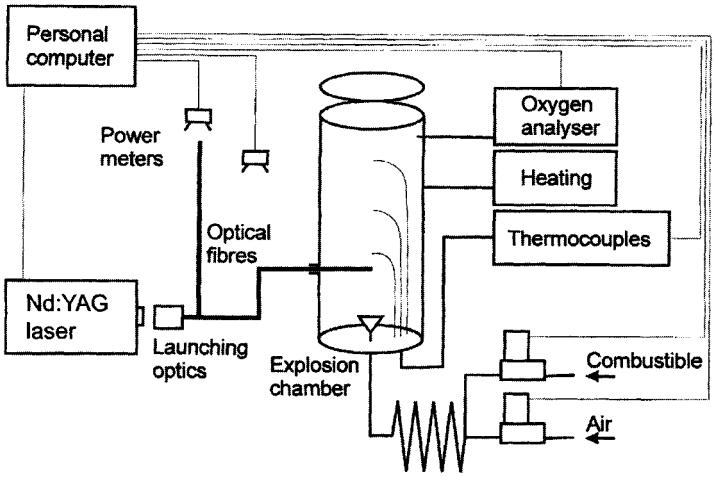

Figure 2–49 Experimental apparatus used for determining critical data for ignition of a wide range of explosive gases and vapors mixed with air by optical radiation absorbed by a solid iron/manganse oxide target attached to the end of an optical fiber. From Welzel et al. (2000).

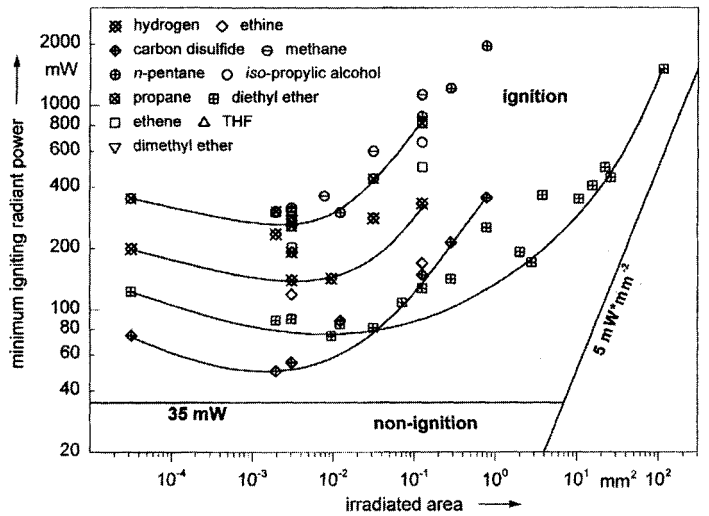

Figure 2–50 Minimum radiant power (mW) for ignition as a function of the surface area of the iron/manganese target (mm^2) for a range of explosive mixtures of combustible gases/vapors and air. From Welzel et al. (2000).

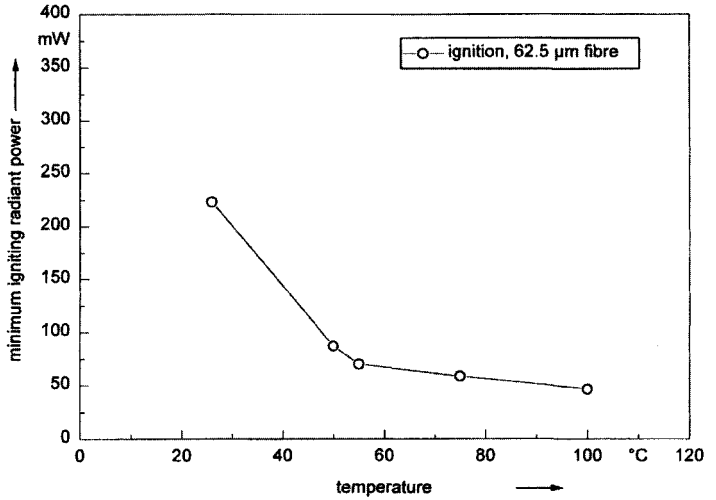

Figure 2–51 Minimum radiant power required for igniting a mixture of 12 vol.% diethyl ether in air, as a function of the temperature of the explosive mixture. The heated target was a thin layer of black iron/manganese oxide attached to an optical fiber of diameter 62.5 µm. From Welzel et al. (2000).

generated by X-ray tubes and radioactive substances. Radioactive radiation can heat up a solid surface, owing to internal absorption of radiation energy, to such an extent that the minimum ignition temperature of the surrounding explosive gas mixture is exceeded. Such radiation can also cause direct chemical decomposition of the gas or other chemical reactions which can generate highly reactive radicals or unstable chemical compounds which can lead to ignition.

2.2.10 Concluding Remark

Critical ignition parameters, e.g. the minimum ignition temperature and the minimum ignition energy, of a given explosive gas mixture can vary substantially with the actual ignition source characteristics, and the dynamics, pressure and temperature of the gas mixture. This means that there is a need for methods that permit differentiation when specifying critical parameters for various practical situations. For example, it is essential that the minimum ignition temperature corresponds as closely as possible to the particular industrial situation of concern. The application

Next Page

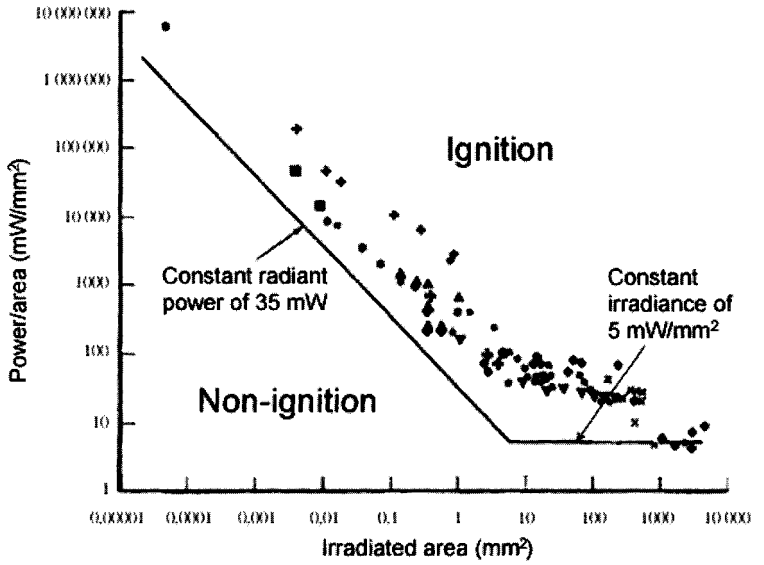

Figure 2–52 Summary of experimental data of minimum radiated power per unit target area (mW/mm²) for igniting a range of explosive mixtures of combustible gases/vapors and air, as a function of the irradiated area (mm²). From Thowle (2000).

of just one value for a given explosive gas, based on a highly conservative laboratory test, irrespective of the actual industrial situation, may in some cases put industry to considerable unnecessary expense.

2.3 Case Histories of Accidental Gas/Vapor Cloud Explosions

2.3.1 Motivation for Section

Experience has shown that "learning by doing" is an effective way of acquiring new knowledge. Unfortunately, this also applies to learning about explosions, which can give rise to much human suffering and grief, as well as material damage and loss of profit. People who have experienced an explosion accident, whether as workers or management in industrial plants, or elsewhere, have a profound appreciation of the realism of this hazard, beyond the reach of those who have only heard or